Exp. Anim. 67(2), 229–237, 2018

—Original—

CRISPR-Cas9-mediated generation of obese and diabetic mouse models

Jae-il ROH[1)]*, Junghoon LEE[2)]*, Seong Uk PARK[1)], Young-Shin KANG[2)], Jaehoon LEE[1)], Ah-Reum OH[2)], Dong Joon CHOI[1)], Ji-Young CHA[2)], and Han-Woong LEE[1)]

[1)]*Department of Biochemistry, College of Life Science and Biotechnology and Yonsei Laboratory Animal Research Center, Yonsei University, 50 Yonsei-ro, Seodaemun-gu, Seoul 03722, Republic of Korea*
[2)]*Department of Biochemistry, Lee Gil Ya Cancer and Diabetes Institute, GAIHST, Gachon University College of Medicine, 155 Gaetbeol-ro, Yeonsu-gu, Incheon 21999, Republic of Korea*

Abstract: Mouse models of obesity (*ob*/*ob*) and diabetes (*db*/*db*) in which the leptin (*Lep*) and leptin receptor (*Lepr*) genes have been mutated, respectively, have contributed to a better understanding of human obesity and type 2 diabetes and to the prevention, diagnosis, and treatment of these metabolic diseases. In this study, we report the first CRISPR-Cas9-induced *Lep* and *Lepr* knockout (KO) mouse models by co-microinjection of Cas9 mRNA and sgRNAs that specifically targeted *Lep* or *Lepr* in C57BL/6J embryos. Our newly established *Lep* and *Lepr* KO mouse models showed phenotypic disorders nearly identical to those found in *ob*/*ob* and *db*/*db* mice, such as an increase in body weight, hyperglycemia, and hepatic steatosis. Thus, Cas9-generated *Lep* and *Lepr* KO mouse lines will be easier for genotyping, to maintain the lines, and to use for future obesity and diabetes research.

Key words: CRISPR-Cas9, *db*/*db*, leptin, leptin receptor, *ob*/*ob*

Introduction

Obesity and type 2 diabetes are two of the risk factors of death worldwide [19] and represent significant economic burden. Because the incidence of these diseases continually increasing, the predicted cost for treating them is expected to rise to $48 billion per year by the year 2030 [32]. Additionally, comorbidities including hypertension, hyperlipidemia, and cancer represent significant economic burden and loss of life quality [13], making metabolic disorders a significant public health concern. Therefore, the identification of new methods for disease prevention, diagnosis, and cure is critical. New animal models of metabolic disease are being continually developed in an effort to unravel the mechanism of action behind several genes and functional pathways implicated in the development of metabolic disorders and will prove powerful tools for understanding obesity and diabetes pathology, as well as for developing new treatments and preventive approaches.

There are five obesity-related loci in mouse models of metabolic disease; of these five, the obese (*ob*) and

(Received 2 October 2017 / Accepted 7 December 2017 / Published online in J-STAGE 16 January 2018)

**These authors contributed equally.*

Addresses corresponding: H.-W. Lee, Department of Biochemistry, College of Life Science and Biotechnology and Yonsei Laboratory Animal Research Center, Yonsei University, 50 Yonsei-ro, Seodaemun-gu, Yonsei University, Seoul 03722, Republic of Korea
J.-Y. Cha, Department of Biochemistry, Lee Gil Ya Cancer and Diabetes Institute, GAIHST, Gachon University College of Medicine, 155 Gaetbeol-ro, Yeonsu-gu, Incheon 21999, Republic of Korea

Supplementary Figures and Table: refer to J-STAGE: https://www.jstage.jst.go.jp/browse/expanim

This is an open-access article distributed under the terms of the Creative Commons Attribution Non-Commercial No Derivatives (by-nc-nd) License <http://creativecommons.org/licenses/by-nc-nd/4.0/>.

©2018 Japanese Association for Laboratory Animal Science

diabetes (*db*) loci are the most commonly investigated [9]. The genes at these two loci were identified as leptin (*Lep)* and leptin receptor (*Lepr*) in 1994 and 1996, respectively [3, 33]. LEP is a 167-amino acid peptide that is primarily produced in white adipose tissues (WAT). Upon entering the bloodstream, signal peptide removal reduces the length of LEP to 147 amino acids [31]. This protein is a key player in regulating energy balance and in body weight control [26]. The brain recognizes the circulating 147 amino acid-long form of leptin through the leptin receptor, which is encoded by the *Lepr* gene [11]. The long *Lepr* isoform, OB-Rb, is mainly expressed in the hypothalamus, while the short isoform, OB-Ra, is expressed throughout the body [8]. Mutations in *Lep* or *Lepr* lead to early-onset obesity and accompanying hyperglycemia with insulin resistance in mice [18], and mutations in *LEP* and *LEPR*, though rare, has been reported in humans [21]. Although the existing *ob*/*ob* and *db*/*db* mouse models have strong, relevant phenotypes and made important contributions to our understanding of metabolic disorders, it is difficult to maintain these lines due to their specific genotyping strategy, which requires additional steps other than PCR [14]. Therefore, the development of easier to maintain obese diabetic mouse lines would represent a significant contribution to metabolic disorder research.

CRISPR-Cas9 is a third-generation engineered nuclease that causes double-strand DNA breaks, eliciting the non-homologous end joining and homologous recombination repair systems [25]. Here, using the CRISPR/Cas9 system, we generate and phenotype *Lep* and *Lepr* knockout (KO) mouse models. These mice are obese and exhibit a diabetic phenotype, even in the first generation, and are phenotypically very similar to the existing *ob*/*ob* and *db*/*db* lines such as gross body weight increasement, hepatic steatosis, and hyperglycemia.

Materials and Methods

In vitro synthesis of Cas9 mRNA and sgRNAs

CRISPR-Cas9 constructs were synthesized as described previously [28]. Briefly, Cas9 mRNA was synthesized *in vitro* from linear DNA templates using the mMESSAGE mMACHINE T7 Ultra kit (Ambion) according to the manufacturer's instructions. DNA templates for sgRNAs were also synthesized *in vitro* using PCR; RNA was synthesized from these templates using a MEGAshortscript T7 kit (Ambion) according to the manufacturer's instructions. The constructs were diluted RNase-free injection buffer (0.25 mM EDTA, 10 mM Tris at pH 7.4) prior to microinjection. Following sequence information was used for sgRNA synthesis; sgRNA#1 of *Lep*, AAGCCACAGGAACCGACACA; sgRNA#2 of *Lep*, TGAGGGTTTTGGTGTCATCC; sgRNA#1 of *Lepr,* GAGTCATCGGTTGTGTTCGG; sgRNA#2 of *Lepr,* AGAAGCCCCCTTCAAAGCCG.

Generation and maintenance of Lep and Lepr KO mouse lines

Lep and *Lepr* KO mouse models were generated using the CRISPR-Cas9 system as described previously [29]. Briefly, CRISPR-Cas9 constructs and sgRNAs were microinjected into fertilized C57BL/6J embryos. Mutations on *Lep* and *Lepr* were confirmed by Sanger sequencing (Cosmo Genetech). Mice were maintained on a normal diet (PicoLab® Rodent Diet 20, Orientbio) under a 12 h light/dark cycle. All animal experiments were performed in accordance with Korean Food and Drug Administration guidelines and protocols were reviewed and approved by the Institutional Animal Care and Use Committee of the Yonsei University (201507-390-01) and Gachon University (2015-0042).

Genotyping of Lep and Lepr KO mouse lines

The genotypes were confirmed by PCR using the following primers; 5′- TCC CAG GGA GGA AAA TGT GCT -3′ (forward for *Lep*), 5′- TGA CAT GTT TCT CAG ACT CTG GTT -3′ (reverse for *Lep*), 5′- CTG CTG GAG CCC CAA ACA ATG C -3′ (forward for *Lepr*), 5′- TTC AAC AAT TGC TTC AGA AGC C -3′ (reverse for *Lepr*). PCR was performed as follows: denaturation at 94°C, 30 cycles of 30 s at 94°C, 30 s at 60°C, and 30 s at 72°C; 7 min at 72°C. Electroporation was conducted on 2–3% of agarose gels and visualized with a Bio-Rad ChemiDoc system.

Mouse management and experiments

At the experimental endpoint, mice were euthanized at the beginning of the light cycle and weighed. Blood samples were collected via the hepatic portal vein, and plasma was obtained by centrifugation at 300 × g for 15 min at 4°C. Livers and gonadal fat were removed, weighed, and either snap-frozen in liquid nitrogen or formalin-fixed. Liver and plasma samples were stored at –80°C until RNA isolation or biochemical analysis. Body composition was assessed by ^{1}H-magnetic reso-

nance spectroscopy (BioSpin, Bruker, Billerica, MA). Mouse lines of *Lep* and *Lepr* KO are available in the Korea Ministry of Food & Drug Safety (*Lep* KO, KNL-HYD-TG0623; *Lepr* KO, KNL-HYD-TG0624).

Hematoxylin and eosin staining

Liver and WAT tissues were fixed in neutral-buffered formalin and embedded in paraffin blocks according to standard procedures, and sections were stained with hematoxylin and eosin (H&E) as described previously [24].

Real-time quantitative PCR

Total RNA was isolated from the liver, brain, and WAT using TRIzol reagent (Ambion), and then cDNA was synthesized using a RevertAid First strand cDNA Synthesis Kit (Thermo). Quantitative gene expression analyses were performed using a CFX384 Real-Time PCR system (Bio-Rad, Berkeley, CA) using SYBR1 Premix Ex TaqTM II, ROX Plus (Takara). Primers used for RT-qPCR were as follows: 5′-AGC TGC AAG GTG CAA GAA GAA-3′ (*Lep* forward), 5′-GGA ATG AAG TCC AAG CCA GTG AC-3′ (*Lep* reverse), 5′-TGA TGT GTC AGA AAT TCT ATG TGG T-3′ (*Lepr* forward), 5′-AGC AAC AGT GGA AGA CTG TTT TG-3′ (*Lepr* reverse), 5′-CAA GAA TAC CAA AGT GCG ATC AA-3′ (*Pparg* forward), 5′-GAG CTG GGT CTT TTC AGA ATA ATA AG-3′ (*Pparg* reverse)'; GGA CAA CAC GCA TTT CAT GAT C-3′ (*Cidea* forward), 5′-GGC TAT TCC CGA TTT CTT TGG-3′ (*Cidea* reverse), 5′-GGA GAT GGC ACA GGA GGA A-3′ (*Cyclophilin* forward), and 5′-GCC CGT AGT GCT TCA GCT T-3′ (*Cyclophilin* reverse).

Biochemical measurements

Blood glucose levels during the glucose tolerance test were measured using Allmedicus, Gluco Dr.^{TM} plus+ (AGM-3000). Plasma insulin and leptin levels were measured using the Mouse Ultrasensitive Insulin ELISA kit (ALPCO, 80-INSMSU-E01) and the Mouse/Rat Leptin ELISA kit (ALPCO, 22-LEPMS-E01), respectively. Homeostasis model assessment IR (HOMA-IR) index was calculated from glucose (mmol/L) X insulin (mU/L)/22.5 [20]. Plasma triglyceride (TG), total cholesterol (T-CHO), high-density lipoprotein cholesterol (HDL), low-density lipoprotein cholesterol (LDL), alanine transaminase (ALT), aspartate transaminase (AST), and lactate dehydrogenase (LDH) levels were determined by automated analysis (Model AU-480; Olympus, Tokyo, Japan) [22].

Statistical analyses

Data were expressed as mean ± standard error of the mean (SEM). Statistical analysis was performed using SPSS (Version 17.0; SPSS Inc., Chicago, IL). Data were analyzed using Kruskal-Wallis tests. Group comparisons were performed with Mann-Whitney *U* tests and corrected with Bonferroni.

Results

Creation of Lep KO mice by Cas9 microinjection

We designed a pair of independent sgRNAs targeting exon 2 of the *Lep* locus to establish a homozygous *Lep* KO mouse model. To minimize off-target sgRNA binding while maximizing target efficiency, we thoroughly analyzed exon 2 of the *Lep* locus using sgRNA designer and CRISPR Design [5, 27] while designing the sgRNAs. Co-injection of the two independent sgRNAs with Cas9 mRNA caused a 79-bp deletion mutation on exon 2 of the *Lep* locus (Fig. 1A), causing a frameshift mutation and exposing a premature stop codon. Compared with the wild type (WT) LEP protein, composed of 167 amino acid residues, the mutant peptide, if translated, encodes only three original amino acid residues and 41 abnormal residues (Fig. 1B). A BLAST search of the abnormal residues revealed no match to known annotated murine proteins, suggesting that the mutant leptin does not function normally. Because the deletion mutation removed a larger portion of the *Lep* locus than in existing *ob*/*ob* mouse models, we were able to confirm the genotype via PCR using a single primer pair (Fig. 1C). Additionally, although we also successfully mutated *both Lep* alleles simultaneously (2- and 77-bp deletion mutations, respectively) in first generation animals, which were severely obese (data not shown), the mice were infertile and therefore the line could not be maintained.

Physiological comparisons of Lep KO and ob/ob mouse models

Due to the premature stop codon exposed by sgRNA-Cas9 mRNA co-injection, we would expect nonsense-mediated mRNA decay [2] and concurrent oblation of gene expression. Indeed, *Lep* mRNA was not detected in WAT in homozygous *Lep* KO mice, but was detected

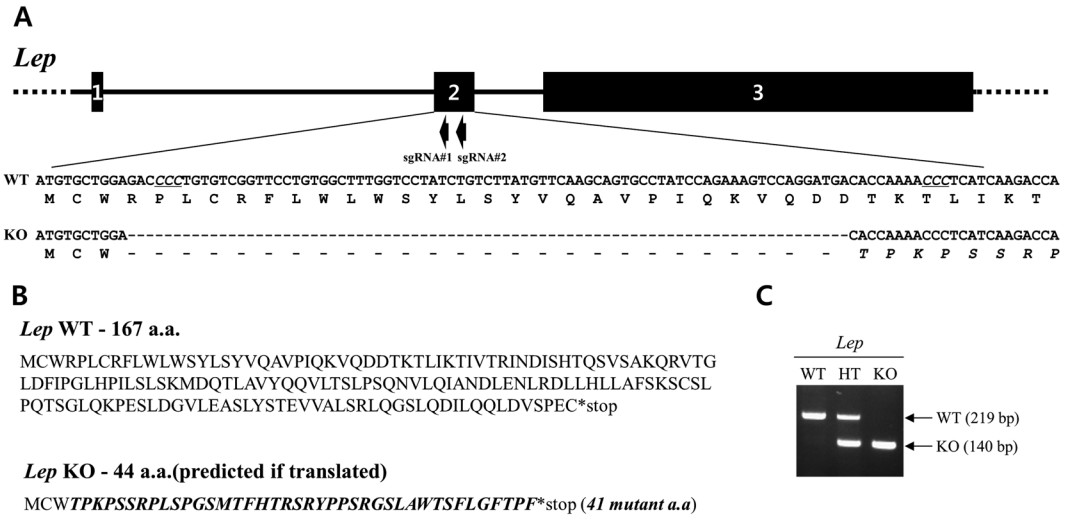

Fig. 1. CRISPR-Cas9-mediated generation of *Lep* KO mice. (A) A representative view of the CRISPR-Cas9 targeting strategy for generating *Lep* KO mice. The *Lep* locus (top panel) and *Lep* nucleotide and amino acid sequences (bottom panel) are shown. Exons are indicated with black boxes and introns are indicated by black lines. The protospacer adjacent motif (PAM) of SpCas9 is italicized and underlined (bottom panel) and mutant amino acids are shown in italics. (B) The length and amino acid sequence of WT *Lep* and the predicted length and amino acid sequence of the mutated form. Italicized amino acids indicate predicted mutant peptides. The asterisk indicates a translation stop signal. (C) PCR genotyping of *Lep* WT (219 bp), heterozygous (219 bp for WT and 140 bp for KO), and KO (140 bp) mice.

in both WT and heterozygous KO mice (Fig. 2A). Phenotypically, the CRISPR-Cas9-generated *Lep* KO mouse is highly comparable to the existing *ob*/*ob* mouse model. At 12 weeks of age, the *Lep* KO mice weigh about 1.8 to 2 times more than WT mice (Figs. 2B and C); similarly, *ob*/*ob* mice are about two times heavier than control mice [4]. Both males and females exhibited drastic changes in gross weight (Figs. 2B, C, and Supplementary Fig. S1A), with a 30% increase in weight at 6 weeks old and a 54% increase in weight at 12 weeks old compared to WT mice (Fig. 2C, Supplementary Fig. S1A). This weight gain compared to WT is likely due to the excessive food intake characterizing the KO animals (Fig. 2D), which is consistent with the *ob*/*ob* phenotype [10]. Although there was no change in lean mass, fat and liver mass increased in the *Lep* KO mice compared to WT (Fig. 2E, Supplementary Figs. S1B and C). Together, these data suggest that the CRISPR-Cas9-induced *Lep* mutation is sufficient to cause obesity in these mice.

Macroscopic and microscopic analyses of the liver and WAT revealed gross morphological changes due to fat accumulation in *Lep* KO mice (Figs. 2F, G, and Supplementary Fig. S1D). The liver was approximately 3-fold larger in *Lep* KO mice compared to WT, and was also a light salmon hue rather than the ruddy color that characterizes normal liver tissue. Consistent with these morphological observations, the two-adipogenic markers peroxisome proliferator-activated receptor gamma (*Pparg)* and cell death-inducing DNA fragmentation factor α-like effector A (*Cidea*) were upregulated in *Lep* KO mice (Supplementary Figs. S1E and F). Plasma levels of the liver damage markers alanine aminotransferase (ALT), aspartate aminotransferase (AST), and lactate dehydrogenase (LDH) were also significantly increased in *Lep* KO mice (Fig. 2H). Plasma TG, T-CHO, LDL, and HDL levels were also markedly higher in *Lep* KO mice (Supplementary Fig. S1G), which is consistent with previous reports on *ob*/*ob* mice [1]. These data therefore suggest that our *Lep* KO mouse model is an efficient model for obesity research as the mice exhibit a strong obesity phenotype with concurrent hepatic steatosis similar to that of *ob*/*ob* mice.

Development of hyperglycemia with insulin resistance in Lep KO mice

In both the *ob*/*ob* and *db*/*db* models, hyperglycemia develops before obesity becomes apparent [23]. We measured blood glucose levels in WT, heterozygous *Lep* KO, and homozygous *Lep* KO mice to determine whether our *Lep* KO mice were hyperglycemic in addition to obese.

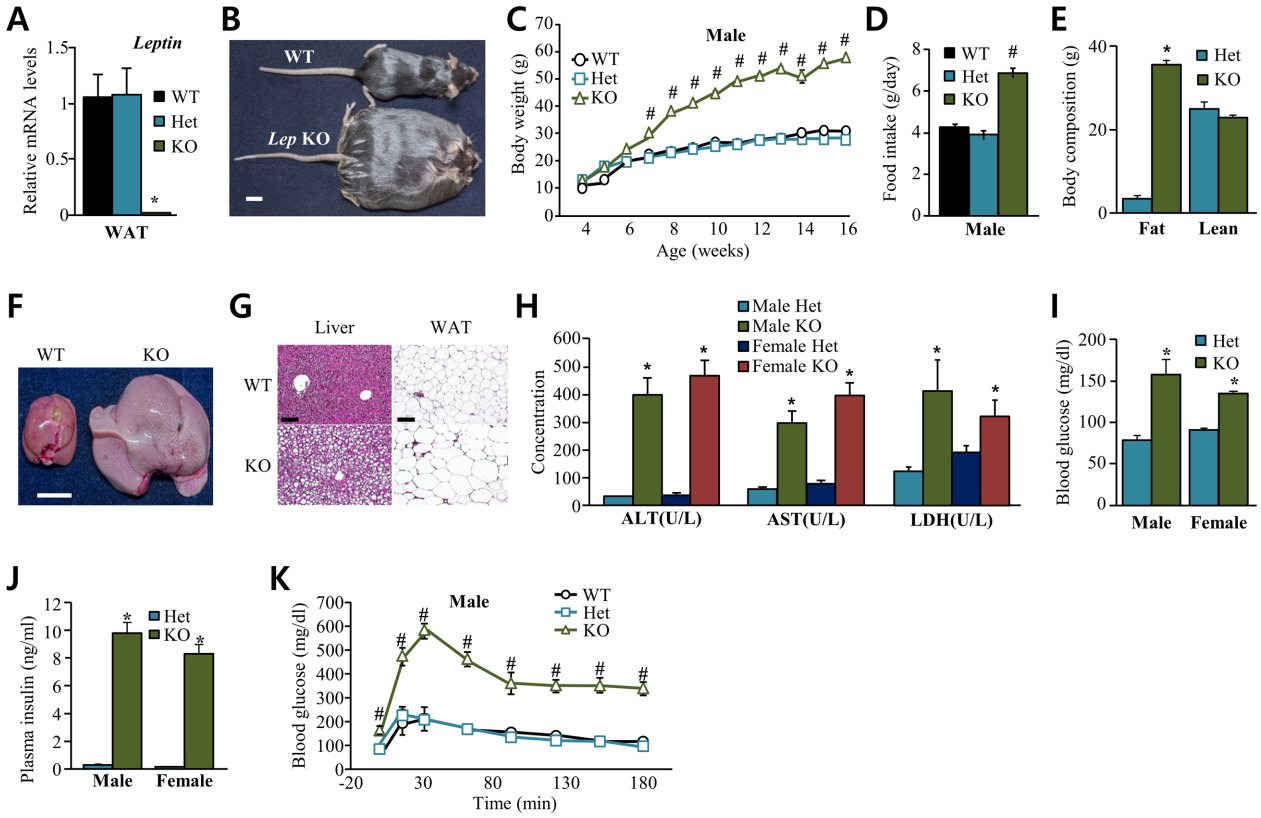

Fig. 2. CRISPR-Cas-9 mediated *Lep* KO causes obesity, hyperglycemia, and hyperinsulinemia. (A) RT-qPCR analysis of *Lep* mRNA levels in the WAT of 10-week-old mice. mRNA levels were normalized to *β-actin*. (B) A representative photograph of 9-month-old mice. Scale bar: 1 cm. (C) Monitoring of body weight over 13 weeks in male mice. The mice were experienced glucose tolerance test at 14 weeks of age. (D) Average daily food intake in 8-week-old mice. (E) Body composition measured by ^{1}H-NMR in 15-week-old male mice. (F, G) Representative image of the macroscopic appearance of livers in 9-month-old mice (F) and H&E staining image of liver and WAT in 16-week-old mice (G). White bar: 1 cm; Black bar: 100 μm. (H) Plasma concentration of ALT, AST, and LDH in male and female mice (ALT: alanine transaminase, AST: aspartate transaminase, LDH: Lactate dehydrogenase). (I, J) Blood glucose (I) and plasma insulin (J) levels in 14-week-old mice after 16 h of fasting. (K) Results of a glucose tolerance test administered in 14-week-old *Lep* WT, heterozygous and homozygous KO male mice fasted for 16 h. Data are presented as the mean ± SEM. WT (n=4), Het (n=5), and *Lep* KO (n=4). Data were analyzed using Kruskal-Wallis test and group comparisons with Mann-Whitney *U* test. $^{\#}P<0.01$ vs. WT and Het group (A, C, D, and K), $^{*}P<0.05$ vs. Het group (E, H–J).

Fasting blood glucose and plasma insulin levels were also significantly increased in *Lep* KO mice compared to heterozygous KO mice (Figs. 2I and J). To quantify the extent of systemic insulin resistance in *Lep* KO mice, *Lep* WT, heterozygous and homozygous KO mice were underwent IPGTT (Fig. 2K and Supplementary Fig. S1H). Fifteen mins after glucose injection, blood glucose levels increased by approximately 2-fold in WT and heterozygous KO mice and increased by 4-fold in homozygous KO mice. Maximal blood glucose levels approached 600 mg/dl in the *Lep* KO mice but remained at levels around 200 mg/dl in WT and heterozygous KO mice. Additionally, analysis of insulin resistance showed significant increment of HOMA-IR index in *Lep* KO mice (Supplementary Fig. S1I). These data indicate that *Lep* KO is associated not only with obesity and hepatic steatosis, but also with hyperglycemia and insulin resistance, like the existing *ob*/*ob* model [31].

Creation of Lepr KO mice by Cas9 microinjection

In a similar approach to that used to generate *Lep* KO mouse, a pair of independent sgRNAs targeting exon 3 of the *Lepr* locus was co-microinjected with Cas9 mRNA to induce a deletion and found the deletion of five nucleotides near binding site for the second sgRNA (Fig. 3A). This deletion caused a frame shift mutation, and exposed premature stop codon. Compared with the WT LEPR protein, which is composed of 1162 amino acid

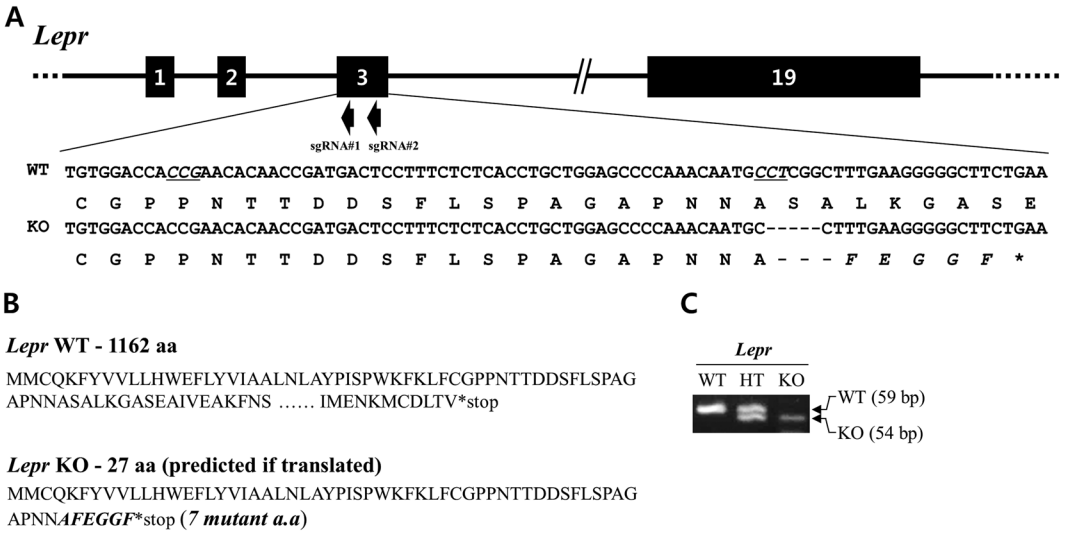

Fig. 3. CRISPR-Cas9-mediated generation of *Lepr* KO mice. (A) A representative view of the CRISPR-Cas9 targeting strategy for generating *Lepr* KO mice. The *Lepr* locus (top panel) and *Lepr* nucleotide and amino acid sequences (bottom panel) are shown. Exons are indicated with black boxes and introns are indicated by black line. The PAM of SpCas9 is italicized and underlined (bottom panel) and mutant amino acids are shown in italics. The asterisk indicates a stop codon. (B) The length and amino acid sequence of WT *Lepr* and the predicted length and amino acid sequence of the mutated form. Italicized amino acids indicate predicted mutant peptides. The asterisk indicates a translation stop signal. (C) PCR genotyping of *Lepr* WT (59 bp), heterozygous (59 bp for WT and 54 bp for KO), and KO (54 bp) mice.

residues, the mutant protein, if translated, encodes only 27 N-terminal amino acid residues (Fig. 3B). Despite the small deletion of only 5 bp, the genotype was successfully confirmed by PCR using only a single primer pair to detect both WT and mutant forms (Fig. 3C).

Depletion of Lepr leads to obesity and liver steatosis

Similar to the *Lep* KO model, oblation of *Lepr* mRNA expression was achieved in the epididymal WAT (eWAT), the liver, and the brain in *Lepr* KO mice (Fig. 4A). Phenotypically, the CRISPR-Cas9-generated *Lepr* KO mouse is highly comparable to the existing *db*/*db* mouse model [10]. The *Lepr* KO mice weigh about 1.8 to 2 times more than WT mice (Figs. 4B and C), which is similar to *db*/*db* [4]. Both males and females exhibited gross changes in body shape and weight compared to control animals (Figs. 4B, C, and Supplementary Fig. S2A), which is likely due to increased food intake by KO mice (Fig. 4D). Liver and WAT are also weighty notably more in *Lepr* KO mice compared to control mice (Fig. 4E and Supplementary Fig. S2B), and liver morphology was severely altered (Fig. 4F). Microscopic and molecular analyses revealed hepatic steatosis with increased expression of adipogenic markers *Pparg* and *Cidea* in the *Lepr* KO livers (Fig. 4G, Supplementary Figs. S2C and D); however, no changes in WAT were observed. Although plasma TG and LDH levels were unchanged, plasma ALT, AST, LDL, HDL, and T-CHO levels were significantly increased in *Lepr* KO mice compared to controls (Fig. 4H and Supplementary Fig. S2E). To compensate for defective leptin receptor in *Lepr* KO mice, plasma leptin levels were significantly increased (Fig. 4I). Together, these data suggest that the CRISPR-Cas9-induced *Lepr* mutation induces obesity.

Development of hyperglycemia with insulin resistance in Lepr KO mice

As with *Lep* KO mice, we measured blood glucose to determine whether *Lepr* KO mice were hyperglycemic compared to WT and heterozygous KO mice. Fasting blood glucose and plasma insulin levels were higher in homozygous KO mice compared to WT or heterozygous KO animals (Figs. 4J and K). To quantify the extent of systemic insulin resistance in *Lepr* KO mice, *Lepr* WT, heterozygous and homozygous KO mice were underwent IPGTT (Fig. 4L). Blood glucose levels of *Lepr* KO mice were significantly higher than *Lepr* WT and heterogyzous mice throughout the course of the experiment.

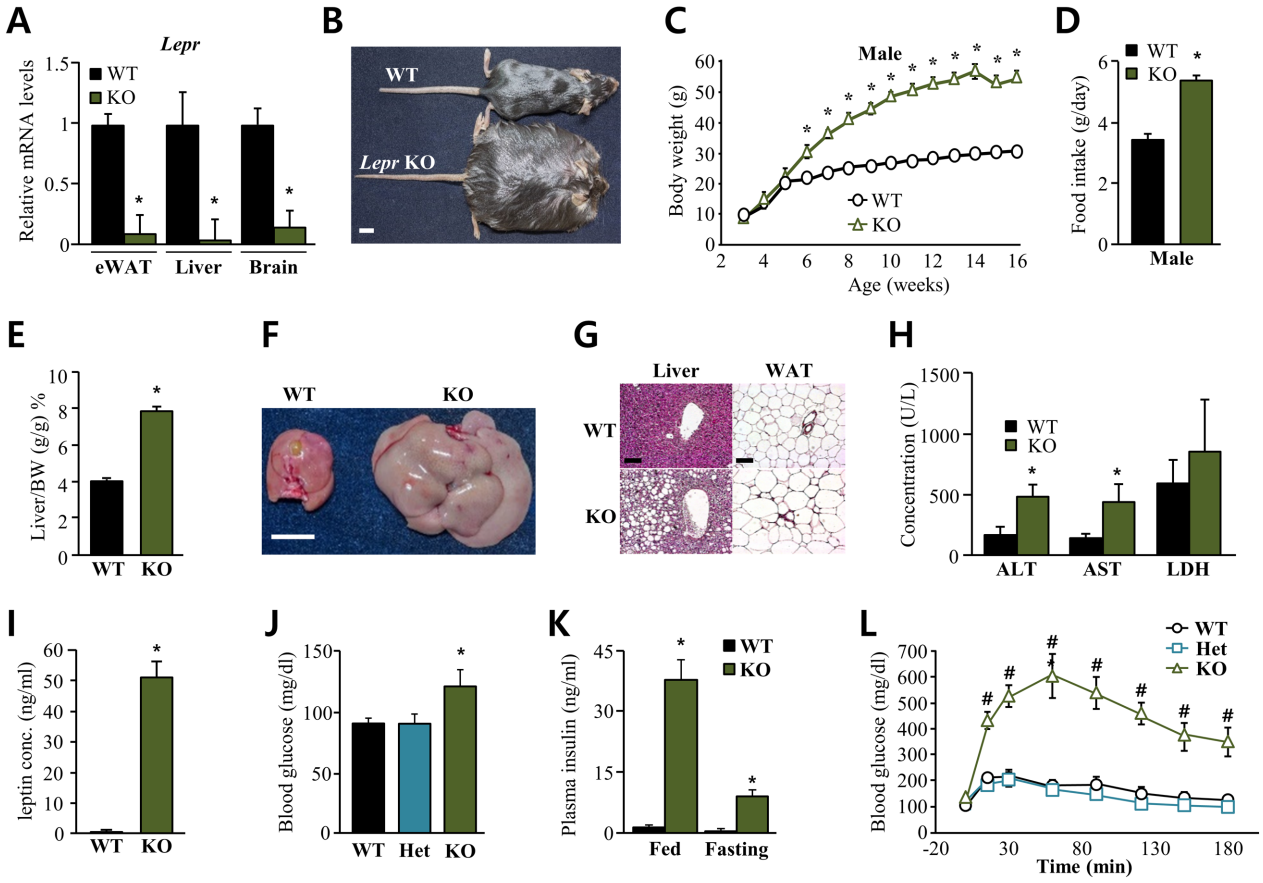

Fig. 4. CRISPR-Cas9-mediated *Lepr* KO causes obesity, glucose intolerance, and hyperinsulinemia. (A) RT-qPCR analysis of *Lepr* mRNA levels in the WAT, liver, and brain of 10-week-old mice. Leptin receptor mRNA levels were normalized to *β-actin*. (B) A representative photograph of 9-month-old mice. (C) Monitoring of body weight over 14 weeks in male mice. The mice were experienced glucose tolerance test at 14 weeks of age. (D) Average daily food intake in 5-week-old male mice. (E) Liver/body weight ratio in 16-week-old male mice. (F) Representative image of the macroscopic appearance of livers in 9-month-old mice. White bar: 1 cm; Black bar: 100 μm. (G) Representative image of liver and WAT H&E staining of 16-week-old male mice. (H) Plasma concentration of ALT, AST, and LDH in 16-week-old WT and *Lepr* KO mice. (I–L) Plasma leptin (I), blood glucose (J), and plasma insulin (K) levels in mice in the fed and fasted (16 h) states. (L) Results of a glucose tolerance test administered in 14-week-old *Lepr* WT, heterozygous and homozygous KO male mice fasted for 16 h. Data are presented as the mean ± SEM. n≥4 individual mice per group. Data were analyzed using Kruskal-Wallis test and group comparisons with Mann-Whitney *U* test. **P*<0.05 vs. WT group (A, C–E, H, I, and K), **P*<0.05 and $^{\#}P$<0.01 vs. WT and Het group (L).

Furthermore, gross enhancement of HOMA-IR index was detected in *Lepr* KO mice (Supplementary Fig. S2F). These data indicate that *Lepr* KO is associated with hyperglycemia, significant glucose intolerance and insulin resistance, identically to the existent *db*/*db* model [17].

Genotyping of Lep and Lepr KO mice generated by Cas9

Even though the genotyping of the *ob*/*ob* and *db*/*db* mouse models can be determined by enzyme restriction, high resolution melting analysis, or a tetra-primer amplification refractory mutation system [7, 14–16, 30], the specific deletion mutations we introduced while generating the *Lep* (79-bp deletion) and *Lepr* (5-bp deletion) KO mouse models help genotyping of these animals, which can be determined via PCR using a single primer pair; the PCR products can be size differentiated using gel electrophoresis (Supplementary Table S1 and Supplementary Fig. S3).

Discussion

Here we describe the successful generation of two alternative *ob*/*ob* and *db*/*db* mouse models using the CRISPR-Cas9 system to induce deletion mutations in

the *Lep* and *Lepr* genes. These models exhibit nearly identical obese and diabetic phenotypes to the existing *ob*/*ob* and *db*/*db* models, yet are easier to genotype and therefore, maintain, making them an attractive model for future metabolic disorder research. *Lep* and *Lepr* mutations have been associated with both obesity and diabetes in humans [6, 12], making our mouse models a relevant tool for understanding metabolic disorders. Notably, the similarity of the disease phenotypes of *Lep* and *Lepr* KO mouse models to those of the *ob*/*ob* and *db*/*db* models was achieved even though the mice are of different genetic backgrounds. Due to these similarities in body weight, hyperglycemia, and insulin resistance, we propose that our mouse models represent a good substitute for the existing *ob*/*ob* and *db*/*db* mouse models.

We hypothesize, due to the success we had using the CRISPR-Cas9 system to effectively target the *Lep* and *Lepr* loci, that the CRISPR-Cas9 system can also be used to target and alter SNPs linked to metabolic diseases, changing them to the WT sequence and thus correcting the problem. For example, a potential approach is CRISPR-Cas9 targeting of mutated loci in pluripotent stem cells isolated from obese patients. Through this, the economic burden associated with diagnosing and treating metabolic disorders may be significantly alleviated through the increased knowledge proffered by using our new obese and diabetic mouse models in investigations of metabolic disorders.

Acknowledgments

This work was supported by grants from the National Research Foundation of Korea (NRF) grants funded by the Korean government (MEST; 2010–0020878, 2012R1A1A2009607, 2015R1A2A1A01003845), the Ministry of Food and Drug Safety (14182MFDS978), a Korea Healthcare Technology R&D Project from the Ministry for Health and Welfare and Family Affairs (A085136) (to H-W Lee), the Ministry of Food and Drug Safety (14182MFDS978), and by the Basic Science Research Program through the National Research Foundation of Korea (NRF) funded by the Ministry of Education, Science and Technology (NRF-2016R1A2B4015866; to J-Y Cha).

References

1. Anstee, Q.M. and Goldin, R.D. 2006. Mouse models in non-alcoholic fatty liver disease and steatohepatitis research. *Int. J. Exp. Pathol.* 87: 1–16. [Medline] [CrossRef]
2. Brogna, S. and Wen, J. 2009. Nonsense-mediated mRNA decay (NMD) mechanisms. *Nat. Struct. Mol. Biol.* 16: 107–113. [Medline] [CrossRef]
3. Chen, H., Charlat, O., Tartaglia, L.A., Woolf, E.A., Weng, X., Ellis, S.J., Lakey, N.D., Culpepper, J., Moore, K.J., Breitbart, R.E., Duyk, G.M., Tepper, R.I., and Morgenstern, J.P. 1996. Evidence that the diabetes gene encodes the leptin receptor: identification of a mutation in the leptin receptor gene in db/db mice. *Cell* 84: 491–495. [Medline] [CrossRef]
4. Coleman, D.L. 1978. Obese and diabetes: two mutant genes causing diabetes-obesity syndromes in mice. *Diabetologia* 14: 141–148. [Medline] [CrossRef]
5. Doench, J.G., Fusi, N., Sullender, M., Hegde, M., Vaimberg, E.W., Donovan, K.F., Smith, I., Tothova, Z., Wilen, C., Orchard, R., Virgin, H.W., Listgarten, J., and Root, D.E. 2016. Optimized sgRNA design to maximize activity and minimize off-target effects of CRISPR-Cas9. *Nat. Biotechnol.* 34: 184–191. [Medline] [CrossRef]
6. Elbaz, R., Dawood, N., Mostafa, H., Zaki, S., Wafa, A., and Settin, A. 2015. Leptin gene tetranucleotide repeat polymorphism in obese individuals in Egypt. *Int. J. Health Sci. (Qassim)* 9: 63–71. [Medline]
7. Ellett, J.D., Evans, Z.P., Zhang, G., Chavin, K.D., and Spyropoulos, D.D. 2009. A rapid PCR-based method for the identification of ob mutant mice. *Obesity (Silver Spring)* 17: 402–404. [Medline] [CrossRef]
8. Fei, H., Okano, H.J., Li, C., Lee, G.H., Zhao, C., Darnell, R., and Friedman, J.M. 1997. Anatomic localization of alternatively spliced leptin receptors (Ob-R) in mouse brain and other tissues. *Proc. Natl. Acad. Sci. USA* 94: 7001–7005. [Medline] [CrossRef]
9. Friedman, J.M. and Leibel, R.L. 1992. Tackling a weighty problem. *Cell* 69: 217–220. [Medline] [CrossRef]
10. Friedman, J.M. 1997. Leptin, leptin receptors and the control of body weight. *Eur. J. Med. Res.* 2: 7–13. [Medline]
11. Funahashi, H., Yada, T., Suzuki, R., and Shioda, S. 2003. Distribution, function, and properties of leptin receptors in the brain. *Int. Rev. Cytol.* 224: 1–27. [Medline] [CrossRef]
12. Funcke, J.B., von Schnurbein, J., Lennerz, B., Lahr, G., Debatin, K.M., Fischer-Posovszky, P., and Wabitsch, M. 2014. Monogenic forms of childhood obesity due to mutations in the leptin gene. *Mol Cell Pediatr* 1: 3. [Medline] [CrossRef]
13. Grundy, S.M. and Barnett, J.P. 1990. Metabolic and health complications of obesity. *Dis. Mon.* 36: 641–731. [Medline]
14. Hirasawa, T., Ohara, T., and Makino, S. 1997. Genetic typing of the mouse ob mutation by PCR and restriction enzyme analysis. *Exp. Anim.* 46: 75–78. [Medline] [CrossRef]
15. Horvat, S. and Bünger, L. 1999. Polymerase chain reaction-restriction fragment length polymorphism (PCR-RFLP) assay for the mouse leptin receptor (Lepr(db)) mutation. *Lab. Anim.* 33: 380–384. [Medline] [CrossRef]
16. Jung, H., Nam, H., and Suh, J.G. 2016. Rapid and efficient identification of the mouse leptin receptor mutation (C57BL/

KsJ-db/db) by tetra-primer amplification refractory mutation system-polymerase chain reaction (ARMS-PCR) analysis. *Lab. Anim. Res.* 32: 70–73. [Medline] [CrossRef]
17. Koranyi, L., James, D., Mueckler, M., and Permutt, M.A. 1990. Glucose transporter levels in spontaneously obese (db/db) insulin-resistant mice. *J. Clin. Invest.* 85: 962–967. [Medline] [CrossRef]
18. Lutz, T.A. and Woods, S.C. 2012. Overview of animal models of obesity. *Curr. Protoc. Pharmacol.* Chapter 5: Unit5 61.
19. Mathers, C.D. and Loncar, D. 2006. Projections of global mortality and burden of disease from 2002 to 2030. *PLoS Med.* 3: e442. [Medline] [CrossRef]
20. Matthews, D.R., Hosker, J.P., Rudenski, A.S., Naylor, B.A., Treacher, D.F., and Turner, R.C. 1985. Homeostasis model assessment: insulin resistance and beta-cell function from fasting plasma glucose and insulin concentrations in man. *Diabetologia* 28: 412–419. [Medline] [CrossRef]
21. O'Rahilly, S. 2009. Human genetics illuminates the paths to metabolic disease. *Nature* 462: 307–314. [Medline] [CrossRef]
22. Oh, A.R., Bae, J.S., Lee, J., Shin, E., Oh, B.C., Park, S.C., and Cha, J.Y. 2016. Ursodeoxycholic acid decreases age-related adiposity and inflammation in mice. *BMB Rep.* 49: 105–110. [Medline] [CrossRef]
23. Pelleymounter, M.A., Cullen, M.J., Baker, M.B., Hecht, R., Winters, D., Boone, T., and Collins, F. 1995. Effects of the obese gene product on body weight regulation in ob/ob mice. *Science* 269: 540–543. [Medline] [CrossRef]
24. Roh, J.I., Cheong, C., Sung, Y.H., Lee, J., Oh, J., Lee, B.S., Lee, J.E., Gho, Y.S., Kim, D.K., Park, C.B., Lee, J.H., Lee, J.W., Kang, S.M., and Lee, H.W. 2014. Perturbation of NCOA6 leads to dilated cardiomyopathy. *Cell Reports* 8: 991–998. [Medline] [CrossRef]
25. Sander, J.D. and Joung, J.K. 2014. CRISPR-Cas systems for editing, regulating and targeting genomes. *Nat. Biotechnol.* 32: 347–355. [Medline] [CrossRef]
26. Saxena, N.K., Vertino, P.M., Anania, F.A., and Sharma, D. 2007. leptin-induced growth stimulation of breast cancer cells involves recruitment of histone acetyltransferases and mediator complex to CYCLIN D1 promoter via activation of Stat3. *J. Biol. Chem.* 282: 13316–13325. [Medline] [CrossRef]
27. Slaymaker, I.M., Gao, L., Zetsche, B., Scott, D.A., Yan, W.X., and Zhang, F. 2016. Rationally engineered Cas9 nucleases with improved specificity. *Science* 351: 84–88. [Medline] [CrossRef]
28. Sung, Y.H., Jin, Y., Kim, S., and Lee, H.W. 2014. Generation of knockout mice using engineered nucleases. *Methods* 69: 85–93. [Medline] [CrossRef]
29. Sung, Y.H., Kim, J.M., Kim, H.T., Lee, J., Jeon, J., Jin, Y., Choi, J.H., Ban, Y.H., Ha, S.J., Kim, C.H., Lee, H.W., and Kim, J.S. 2014. Highly efficient gene knockout in mice and zebrafish with RNA-guided endonucleases. *Genome Res.* 24: 125–131. [Medline] [CrossRef]
30. Sutter, A.G., Palanisamy, A.P., Kurtz, N., Spyropoulos, D.D., and Chavin, K.D. 2013. Efficient method of genotyping ob/ob mice using high resolution melting analysis. *PLoS One* 8: e78840. [Medline] [CrossRef]
31. Wang, B., Chandrasekera, P.C., and Pippin, J.J. 2014. Leptin- and leptin receptor-deficient rodent models: relevance for human type 2 diabetes. *Curr. Diabetes Rev.* 10: 131–145. [Medline] [CrossRef]
32. Wang, Y.C., McPherson, K., Marsh, T., Gortmaker, S.L., and Brown, M. 2011. Health and economic burden of the projected obesity trends in the USA and the UK. *Lancet* 378: 815–825. [Medline] [CrossRef]
33. Zhang, Y., Proenca, R., Maffei, M., Barone, M., Leopold, L., and Friedman, J.M. 1994. Positional cloning of the mouse obese gene and its human homologue. *Nature* 372: 425–432. [Medline] [CrossRef]